

This is the peer reviewed version of an accepted journal article – ‘Differential pharmacokinetics and pharmacokinetic/pharmacodynamic modelling of robenacoxib and ketoprofen in a feline model of inflammation’ – which has been published in final form at <http://dx.doi.org/10.1111/jvp.12107>.

This draft has been made available on the RVC’s Open Access publications repository in accordance with the College’s Open Access policy.

This article may be used for non-commercial purposes in accordance with the publisher’s self-archiving policy, which can be found at <http://olabout.wiley.com/WileyCDA/Section/id-820227.html>.

The full details of the published version of the article are as follows:

TITLE: Differential pharmacokinetics and pharmacokinetic/pharmacodynamic modelling of robenacoxib and ketoprofen in a feline model of inflammation

AUTHORS: Pelligand, L and King, J N and Hormazabal, V and Toutain, P L and Elliott, J and Lees, P

JOURNAL TITLE: Journal of Veterinary Pharmacology and Therapeutics

VOLUME/EDITION: 37/4

PUBLISHER: Wiley

PUBLICATION DATE: August 2014

DOI: 10.1111/jvp.12107

1 **Differential pharmacokinetics and pharmacokinetic/pharmacodynamic**
2 **modelling of robenacoxib and ketoprofen in a feline model of inflammation**

3 L. PELLIGAND*

4 J.N. KING†

5 V. HORMAZABAL‡

6 P.L. TOUTAIN§

7 J. ELLIOTT*

8 P. LEES*

9

10 **Department of Comparative and Basic Sciences, Royal Veterinary College, Hawkshead*
11 *Campus, Hatfield, Hertfordshire, UK; †Novartis Animal Health Inc., Clinical Development,*
12 *Basel, Switzerland (J.N.K.); ‡Department of Food Safety and Infection Biology, The Norwegian*
13 *School of Veterinary Science, Oslo, Norway (V.H.); §UMR 1331 Toxalim INRA/INP/UPS. Ecole*
14 *Nationale Vétérinaire de Toulouse, Toulouse, France (P.L.T.)*

15 *Corresponding author: Ludovic Pelligand, Department of Comparative and Basic Sciences,*
16 *Royal Veterinary College, Hawkshead Campus, Hatfield, Hertfordshire, UK. Email:*
17 *lpelligand@rvc.ac.uk*

18 Short title: robenacoxib and ketoprofen in the cat

19 Key words: Robenacoxib, NSAIDs, feline, tissue cage, PK/PD

20

21 ABSTRACT

22 Robenacoxib and ketoprofen are acidic non-steroidal anti-inflammatory drugs (NSAIDs). Both
23 are licensed for once daily administration in the cat, despite having short blood half-lives. This
24 study reports the pharmacokinetic/pharmacodynamic (PK/PD) modelling of each drug in a feline
25 model of inflammation. Eight cats were enrolled in a randomised, controlled, three period cross-
26 over study. In each period, sterile inflammation was induced by injection of carrageenan into a
27 subcutaneously implanted tissue cage, immediately before the subcutaneous injection of
28 robenacoxib (2 mg/kg), ketoprofen (2 mg/kg) or placebo. Blood samples were taken for
29 determination of drug and serum thromboxane (Tx)B₂ concentrations (measuring COX-1
30 activity). Tissue cage exudate samples were obtained for drug and prostaglandin(PG)E₂
31 concentrations (measuring COX-2 activity). Individual animal pharmacokinetic and
32 pharmacodynamic parameters for COX-1 and COX-2 inhibition, were generated by PK/PD
33 modelling. S(+) ketoprofen clearance scaled by bioavailability (CL/F) was 0.114 L/kg/h
34 (elimination half-life =1.62 h). For robenacoxib, blood CL/F was 0.684 L/kg/h (elimination half-
35 life =1.13 h). Exudate elimination half-lives were 25.9 and 41.5 h for S(+) ketoprofen and
36 robenacoxib, respectively. Both drugs reduced exudate PGE₂ concentration significantly between
37 6 and 36 h. Ketoprofen significantly suppressed (>97%) serum TxB₂ between 4 min and 24 h,
38 whereas suppression was mild and transient with robenacoxib. *In vivo* IC₅₀COX-1/IC₅₀COX-2
39 ratios were 66.9:1 for robenacoxib and 1:107 for S(+) ketoprofen. The carboxylic acid nature of
40 both drugs may contribute to the prolonged COX-2 inhibition in exudate, despite short half-lives
41 in blood.

42 INTRODUCTION

43 Non-steroidal anti-inflammatory drugs (NSAIDs) inhibit cyclooxygenase (COX) and have been
44 used for many decades to alleviate inflammation-related pain in human and veterinary medicine.
45 COXibs belong to a class of NSAIDs that selectively inhibit the COX isoform up-regulated in
46 inflammation (COX-2), with much less inhibition of the constitutively expressed COX isoform
47 (COX-1) responsible for the production of so-called “housekeeping” eicosanoids. Several
48 COXibs were associated with an increased risk of myocardial infarction or stroke in man when
49 evaluated against non-selective NSAID comparators and administered at recommended dose
50 rates (Bombardier *et al.*, 2000; Silverstein *et al.*, 2000). However, lumiracoxib contrasted with
51 other COXibs by displaying favourable cardiovascular and gastrointestinal safety profiles in a
52 study incorporating more than 18,000 human patients (Farkouh *et al.*, 2004).

53
54 Despite a short plasma half-life (2 to 6.5 h) in man, lumiracoxib was authorised for once daily
55 administration (Mysler, 2004), whereas rofecoxib and celecoxib were both administered twice
56 daily, despite their long respective half-lives of 17 and 19 to 32 h (Vasquez-Bahena *et al.*, 2010).
57 The persistent clinical efficacy of lumiracoxib may be related to a prolonged residence of the
58 drug in inflamed joints (Scott *et al.*, 2004; Brune & Furst, 2007).

59
60 Robenacoxib is a structural analogue of lumiracoxib, licensed for use in cats (and dogs). Both
61 drugs are structurally related to diclofenac (Fig. 1), containing a carboxylic acidic function
62 instead of the methylsulphone (as for rofecoxib) or the sulphonamide (as for celecoxib) groups
63 characteristic of first generation COXibs. Robenacoxib has a short blood half-life of 1.9 h after

64 subcutaneous administration in the cat (Pelligand *et al.*, 2012b) but is as effective as an analgesic
65 as meloxicam (half-life 37 h) for at least 22 h post-operatively (Kamata *et al.*, 2012).

66

67 Ketoprofen is a COX-1 selective NSAID (Fig. 1), licensed for once daily administration in man
68 and cats (Warner *et al.*, 1999; Schmid *et al.*, 2010) despite short elimination half-lives for the
69 enantiomer S(+) ketoprofen of 1.2 h in the cat and 2 to 3 h in man (Rudy *et al.*, 1998; Lees *et al.*,
70 2003).

71 We hypothesised that robenacoxib and ketoprofen would be similarly effective as anti-
72 inflammatory drugs in a feline model of inflammation, despite the differences in COX
73 selectivity, because of similar concentration-time profiles and potency for COX-2 inhibition.
74 Several models of inflammation have been developed in the cat (Giraudel *et al.*, 2005b;
75 Pelligand *et al.*, 2012a) but only the carrageenan-based tissue cage model of Pelligand *et al.*
76 (2012a) allows serial measurement of NSAID concentrations in blood and at the site of
77 inflammation, as well as determination of the magnitude and time-profiles of COX-1 and COX-2
78 inhibition. We have previously described exudate sampling from these cages for serial
79 measurement of NSAID and Prostaglandin(PG)E₂ concentrations, the latter inflammatory
80 mediator as a surrogate of COX-2 activity, together with blood sampling for measurement of
81 serum thromboxane(Tx)B₂ as a surrogate of COX-1 activity (Pelligand *et al.*, 2012a; Pelligand *et*
82 *al.*, 2012b). The model further enables calculation of pharmacodynamic parameters of NSAIDs,
83 namely I_{max} (efficacy), IC₅₀ (potency) and n (slope of the concentration-effect relationship).
84 These parameters are used to calculate dosage regimens for clinical use (Lees *et al.*, 2004).

85

86 The aims of this study were to: (i) compare the pharmacokinetic and the pharmacodynamic
87 profiles of robenacoxib and ketoprofen in feline blood and exudate; (ii) compare *in vivo* IC₅₀
88 COX-2, *ex vivo* IC₅₀ COX-1 and COX inhibition selectivity for each drug; and (iii) compare and
89 contrast the pharmacokinetic and pharmacodynamic profiles of two carboxylic acid sub-groups
90 of NSAIDs, the profens and COXibs, in the cat.

91

92 MATERIALS AND METHODS

93 *Animals*

94 Eight domestic short hair cats (all neutered, 5 males and 3 females, aged 1 to 3 years), weighing
95 4.0 ± 0.39 kg, were enrolled into the study after an acclimatisation period of one month. Health
96 checks were performed before the start of each sampling period. Between study periods, the cats
97 were grouped housed altogether. They were fed a dry commercial diet (RF23, Royal Canin,
98 Aimargues, France) in two equal portions daily, based on their metabolic requirements. Drinking
99 water was available *ad libitum*. The room was lit from 7.00 am to 7.00 pm.

100

101 The study complied with United Kingdom Home Office regulations (Project License Number
102 70/6132). The protocol was approved by the Royal Veterinary College Ethics and Welfare
103 Committee. All tissue cages were electively removed under general anaesthesia 6 months after
104 implantation, before the cats were re-homed, as no long lasting sequelae resulted from the
105 protocol.

106

107 *Animal preparation and induction of inflammation*

108 Four tissue cages were implanted surgically in each cat, as previously described (Pelligand *et al.*,
109 2012b). Briefly, medical grade silicone cylindrical tissue cages (SF Medical, Fresno, CA, USA)
110 were prepared to the following dimensions: 70 mm length, 15.9 mm external diameter, 12.7 mm
111 internal diameter (6.7 cm³ internal volume) with 12 holes at each pole providing a total surface
112 exchange area of 3.0 cm² per cage. They were sterilised and surgically inserted subcutaneously,
113 under isoflurane (IsoFlo, Abbott Animal Health, Maidenhead, UK) general anaesthesia, parallel
114 to the vertebral column in the flank and thorax areas. Analgesia was provided intra- and post-
115 operatively as described by Pelligand *et al.* (2012a). The tissue cages were flushed with sterile
116 saline under general anaesthesia 7 weeks after implantation to remove any remaining cellular
117 debris and subsequently used experimentally, not earlier than 10 weeks after implantation. On
118 the day before dosing, the fur over the cages was clipped and a double-lumen catheter
119 (CS15402E, Arrow International Ltd, Uxbridge, UK) was inserted in a jugular vein under
120 general anaesthesia (Pelligand *et al.* 2012a).

121

122 On day 1 of each period, 1 mL of a 2% sterile carrageenan solution (Viscarin, FMC biopolymers,
123 Philadelphia, PA, USA) was injected into a naïve tissue cage (Pelligand *et al.*, 2012b) and this
124 tissue cage was used to harvest exudate in that period. A different tissue cage was stimulated for
125 each subsequent period.

126

127 *Experimental design*

128 The experiment was conducted as a three-period, three-sequence, cross-over with 28 day
129 washout intervals. The treatment for the first period was allocated following a randomised
130 blocked design and the sequence of treatments for the subsequent periods followed an

131 incomplete latin square design. All cats received each of the treatments. The three treatments,
132 administered subcutaneously in the neck area, were: robenacoxib 2 mg/kg (Onsior 2.0% solution,
133 Novartis Animal Health, Basel, Switzerland); racemic ketoprofen 2 mg/kg (Ketofen 1% solution,
134 Merial Animal Health, Harlow, Essex, UK); and 0.9% saline (0.1 mL/kg) as placebo. On each
135 test day, the cats were fed 2 h before dosing and again after the final blood sample of the day (12
136 h after dosing). The carrageenan-stimulated cages were sampled (1.0 to 1.3 mL of exudate on
137 each occasion) before and at 3, 6, 9, 12, 24, 34, 48, 72, 96 and 120 h after carrageenan injection
138 (11 serial samples from the same cage). Samples were transferred immediately to 1.5 mL
139 Eppendorf tubes containing 10 µg indomethacin (Sigma Aldrich, Poole, Dorset, UK) to prevent
140 artefactual *ex vivo* eicosanoid generation. The tube was mixed by gentle inversion and placed on
141 ice until centrifugation at 1000 g, 4° C for 10 min. The supernatant was aliquoted and frozen at -
142 80°C prior to measurement of exudate PGE₂ and concentrations of ketoprofen or robenacoxib.

143

144 Blood samples (maximum 1.5 mL per sample) were taken from the distal port jugular catheter
145 before dosing and at 4, 15, 30 min, then 1, 1.5, 2, 3, 4, 6, 9, 12, 24 and 48 h after dosing. An
146 aliquot of each blood sample (0.2 mL) was allowed to clot in a glass tube (Chromacol, Welwyn
147 Garden City, Herts., UK) whilst incubated in a water bath at 37° C for 1 h then centrifuged (1500
148 g, 4° C, 10 min) and the supernatant stored at -80° C prior to measurement of serum TxB₂. The
149 remainder of the sample (1.3 mL) was transferred into an EDTA tube (International Scientific
150 Supplies Ltd., Bradford, Yorks., UK) for blood robenacoxib measurement or a heparin tube for
151 plasma ketoprofen measurement and stored at -80° C.

152

153 To ensure accuracy of pharmacokinetic calculations, cats were weighed on the day of catheter
154 placement, actual injected doses were calculated by weighing syringes before and after injection
155 and actual rather than nominal times of blood sampling were used.

156

157 *Measurement of NSAID concentrations*

158 Plasma (ketoprofen), blood (robenacoxib) and exudate (both drugs) were spiked with known
159 drug concentrations to establish standard curves, and quality controls (QCs) were prepared and
160 dispersed over the sequence of unknown samples, to monitor the overall performance of each
161 analytical method. The percentage of back-calculated concentrations of standards within $\pm 15\%$
162 of their nominal value and the percentage of QCs within $\pm 15\%$ of their theoretical value were
163 calculated. Imprecision (indicator of between day repeatability) was expressed as the coefficient
164 of variation (CV%) between standard concentrations run on different days. Inaccuracy was
165 expressed as the deviation of the mean (% Relative Error) from the theoretical concentration
166 spiked into blank matrix.

167

168 Robenacoxib concentrations in feline blood were measured using a sensitive analytical method,
169 as described by Jung *et al.* (2009). Briefly, the method involved an initial analysis by HPLC-UV,
170 covering the range of 500-20,000 ng/mL and, if required, a subsequent analysis by LC-MS,
171 covering the range of 3-100 ng/mL for blood. Depending on the results obtained by UV analysis,
172 samples were diluted if necessary in order not to exceed a concentration of 100 ng/mL in the MS
173 method. The same method was used for exudate, except that 250 μL of sample were extracted
174 and diluted two-fold with water, instead of using 500 μL of blood. For blood with the MS
175 method, the lower and upper limits of quantification were 3 and 100 ng/mL, respectively. Since

176 the exudate was diluted two fold, the MS method had a range of 6-200 ng/mL for exudate in the
177 initial method validation, but this was extended subsequently to 3.5 – 200 ng/mL, as it was
178 established during the analysis that reliable results were obtained at the lower end of the range.
179 For robenacoxib, inaccuracy was less than 10.4% and imprecision was less than 9.3%.

180

181 R(-) ketoprofen and S(+) ketoprofen concentrations were measured in exudate and plasma by
182 liquid chromatography mass-spectrometry (API 2000 LC/MS/MS system, Applied Biosystems,
183 Ontario, Canada). The method, previously validated for cat and piglet plasma (Fosse *et al.*, 2011
184 and Hormazábal, unpublished data), had lower and upper limits of quantification of 10 and 8,000
185 ng/mL for both matrices. After extraction, filtration and centrifugation of 0.5 mL
186 plasma/exudate, 50 µL of the supernatant was separated on a 100 x 4.6 mm Chirobiotic R
187 column packed with 5 µm ristocetin A particles (Chirobiotic R, Astec, NJ, USA) at 18°C. The
188 mobile phase comprised 46% of 10 mM ammonium acetate (containing 0.3% formic acid) and
189 54% methanol. Flow rate was 0.6 mL/min. A guard column with similar sorbent was used (20 x
190 4.0mm). Average retention times were 4.9 and 5.4 min for S(+) and R(-) ketoprofen,
191 respectively. The detector operated in multiple reactions monitoring (MRM) mode and collected
192 ion data in positive mode. The protonated molecular ion was m/z 255. The product ion m/z 209.1
193 was used for screening and quantification, while the ratios with the product ion m/z 105.2 were
194 used for confirmation of the identity. For ketoprofen enantiomers, inaccuracy was less than 1.3%
195 and imprecision was less than 0.7%.

196

197 *Pharmacodynamic measurements*

198 *In vivo* generation of exudate PGE₂ and *ex vivo* generation of serum TxB₂ were used as
199 surrogates for COX-2 and COX-1 activities, respectively. Although the main source of TxB₂ in
200 serum is platelet COX-1, a minor contribution from COX-2 or from other cells cannot be
201 completely excluded. Additionally, COX-1 may contribute to the synthesis of PGE₂ in exudate
202 (Nantel *et al.*, 1999; Wallace *et al.*, 1999), but the magnitude of this production is likely to be
203 negligible, based on the fact that COX-1 is not induced in carrageenan inflammatory models
204 (Tomlinson *et al.*, 1994).

205

206 Serum TxB₂ and exudate PGE₂ concentrations were measured with competitive radio-
207 immunoassays, adapted from Higgins *et al.* (1984) as described in a previous validation paper
208 (Pelligand *et al.*, 2012a). Two concentrations of pooled samples were aliquoted, and used as
209 quality controls, dispersed over the sequences of unknown samples to calculate inter- and intra-
210 assay variability. Exudate PGE₂ intra-assay variability was 3% for the high control concentration
211 (2.9 ng/mL) and 23.9% for the low control concentration (0.13 ng/mL). Inter-assay variability
212 was 2.1% for the high control and 31% for the low control concentrations. Serum TxB₂ intra-
213 assay variability was 7.2% for the high control (235.1 ng/mL) and 13.2% for the low control
214 (56.5 ng/mL) concentrations. Inter-assay variability was 2.3% and 11.3% for the high and low
215 control concentrations, respectively. All validation data complied with analytical
216 recommendations guidelines (Kelley & DeSilva, 2007; Viswanathan *et al.*, 2007) except for
217 PGE₂ inter-assay variability. Therefore, all samples from the same cats were always analysed in
218 the same batch.

219

220 *Pharmacokinetic data analysis*

221 Pharmacokinetics and PK/PD modelling were performed by the least-squares regression method,
222 using commercial software (WinNonlin version 5.2, Pharsight Corporation, Mountain View, CA,
223 USA). Goodness of fit and selection of the appropriate model were evaluated using the Akaike
224 Information Criterion estimate (Yamaoka *et al.*, 1978) and by visual inspection of the fitted
225 curves and residuals.

226 Blood robenacoxib and plasma ketoprofen enantiomer concentrations $C(t)$ were fitted for each
227 cat using an equation corresponding to drug disposition in a two-compartmental model with
228 absorption phase (subcutaneous administration, Eq. 1):

$$229 \quad C(t) = -(Y_1 + Y_2) \cdot e^{-k_a \cdot (t-t_{lag})} + Y_1 \cdot e^{-\lambda_1 \cdot (t-t_{lag})} + Y_2 \cdot e^{-\lambda_2 \cdot (t-t_{lag})} \quad (\text{Eq. 1})$$

230 where λ_1 and λ_2 are the initial and terminal slopes (/h), Y_1 and Y_2 the intercepts on the Y axis
231 (ng/mL), when $C(t)$ is plotted on a semi-logarithmic scale, k_a is the first-order absorption rate
232 constant (/h) and t_{lag} the absorption lag time after subcutaneous administration. Data were
233 weighted by the reciprocal of the estimated value for blood or plasma concentration when
234 necessary.

235
236 Exudate concentrations of robenacoxib or ketoprofen enantiomers $C_e(t)$ were fitted for the data
237 from each cat using an equation corresponding to drug disposition in a bicompartamental model
238 with an absorption phase after dose normalisation (Eq. 2):

$$239 \quad C_e(t) = -(Y_{e1} + Y_{e2}) \cdot e^{-k_{ea} t} + Y_{e1} \cdot e^{-\lambda_{e1} t} + Y_{e2} \cdot e^{-\lambda_{e2} t} \quad (\text{Eq. 2})$$

240 where λ_{e1} and λ_{e2} are the initial and terminal slopes (/h), Y_{e1} and Y_{e2} the intercepts on the Y axis
241 (ng/mL) when $C_e(t)$ is plotted on a semi-logarithmic scale, and k_{ea} is the first-order invasion rate
242 constant in exudate (/h). No weighting was applied to the data for fitting. It was assumed that
243 only a negligible amount of each NSAID gained access to the tissue cage and that the

244 pharmacokinetics in exudate had no effect on the time-course of drug disposition in the rest of
245 the body.

246

247 Pharmacokinetic parameters were generated for robenacoxib (in blood and exudate) and S(+) and
248 R(-) ketoprofen (in plasma and exudate) by non-compartmental analysis for individual cats, as
249 follows: Maximum NSAID concentration, C_{max} , Time of maximum NSAID concentration, T_{max} ,
250 Area under NSAID concentration-time curve, AUC_{0-inf} , Area under first the Moment Curve,
251 $AUMC_{0-inf}$, NSAID Mean Residence Time (MRT) = $AUMC_{0-inf} / AUC_{0-inf}$, NSAID terminal half-
252 life, $t_{1/2} = \ln(2) / \lambda_z$, where λ_z is the slope of the drug elimination phase, computed by linear
253 regression of the logarithmic concentration versus time curve during the elimination phase,
254 NSAID clearance scaled by bioavailability (F), $CL/F = \text{dose} / (F \times AUC_{0-inf})$, where F is the
255 bioavailability for extravascular administration, Apparent volume of distribution of NSAID
256 during the elimination phase, $V_{area}/F = (\text{dose}/F) / (AUC_{0-inf} \times \lambda_z)$.

257

258 *Pharmacodynamic data analysis and PK/PD modelling*

259 A user program was purposely written in WinNonlin for PK/PD modelling. The equations of
260 robenacoxib and S(+) ketoprofen enantiomer disposition in blood/plasma $C(t)$ or in exudate $C_e(t)$
261 were obtained by compartmental pharmacokinetic analysis by fitting equations (1) or (2),
262 respectively, to the observed data. Individual pharmacokinetic parameters were entered as
263 constants to solve the PK/PD models in a 2 stages analysis (Giraudel *et al.*, 2005a).

264 *In vivo* generation of exudate PGE₂ was used as a surrogate for COX-2 activity in order to carry
265 out PK/PD modelling of the NSAIDs in exudate (Lees *et al.*, 2004). An indirect response model
266 described by Pelligand *et al.* (2012b) was used to model the effect of robenacoxib and S(+)

267 ketoprofen on exudate PGE₂ production. The model did not include the R(-) enantiomer, as it
 268 was considered to be devoid of activity on cyclooxygenase at the concentrations achieved.
 269 Indeed, S(+) ketoprofen is the eutomer of the S(+)/R(-) ketoprofen enantiomeric pair (Lees *et al.*,
 270 2003). The response is indirect because it is the consequence of a dynamic physiologic
 271 equilibrium between PGE₂ production after carrageenan injection, the natural clearance of PGE₂
 272 from exudate and the reversible inhibition of COX-2 by NSAIDs, preventing the build-up of
 273 PGE₂ in exudate as in Equation 3 (Dayneka *et al.*, 1993):

$$274 \quad \frac{dPGE_2}{dt} = K_{in}(t) - K_{out} \times PGE_2 \quad (\text{Eq. 3})$$

275 where $dPGE_2/dt$ (ng/mL/h) is the rate of change of PGE₂ concentration in exudate, K_{out} (/h) is a
 276 first order parameter expressing PGE₂ disappearance rate and $K_{in}(t)$ (ng/mL/h) is a zero-order
 277 time-function expressing PGE₂ production rate. K_{in} is considered as a time-dependent parameter,
 278 influenced by carrageenan administration and NSAID concentration (in the periods when
 279 administered). To express the action of carrageenan on K_{in} , a stimulation function (named
 280 $stimul_{PLACEBO}$ and $stimul_{NSAIDs}$ was selected as Eq. 4 and Eq. 5 for the placebo and NSAID
 281 periods, respectively:

$$282 \quad stimul_{PLACEBO} = carrag \times \left(e^{-k_1 \times (t - tlag)} - e^{-k_2 \times (t - tlag)} \right) \quad (\text{Eq. 4})$$

$$283 \quad stimul_{NSAIDs} = carrag \times \left(e^{-k_1 \times (t - tlag2)} - e^{-k_2 \times (t - tlag2)} \right) \quad (\text{Eq. 5})$$

284 where k_1 and k_2 are the first-order rate constants (/h) describing the time-development of the
 285 carrageenan stimulation, $carrag$ is a scalar factor, and $tlag1$ and $tlag2$ represent the delays in the
 286 onset of inflammation for the placebo and NSAID periods, respectively. Consequently, $tlag$ is
 287 the only difference between $stimul_{PLACEBO}$ and $stimul_{NSAIDs}$ function. Equation 4 and Eq. 5

288 assume that the effect of carrageenan stimulation of COX builds up progressively (as reflected
 289 by k_2) after injection, then steadily decreases (as reflected by k_1) (Lepist & Jusko, 2004).

290 It was assumed that robenacoxib and ketoprofen suppressed the carrageenan action in exudate
 291 through an I_{\max} function (Lees *et al.*, 2004) of the form (Eq. 6):

$$292 \quad I(t) = 1 - \frac{I_{\max} \times C_e(t)^n}{IC_{50}^n + C_e(t)^n} \quad (\text{Eq. 6})$$

293 $I(t)$ is a time-dependant scalar. I_{\max} is a scalar fixed to 1, expressing the fact that robenacoxib can
 294 totally inhibit carrageenan pro-inflammatory effect. IC_{50} expresses the NSAID potency against
 295 carrageenan effect; n is the Hill exponent expressing the steepness of the NSAID concentration
 296 versus effect curve. Finally, incorporating Eq. 4 (placebo) or Eq. 5 and Eq. 6 (NSAID) in the
 297 general Eq. 3, the time development of PGE_2 concentration in exudate was described by Eq. 7
 298 (placebo) and Eq. 8 (NSAID):

$$299 \quad \frac{dPGE_2}{dt} = K_{in}(t) - K_{out} \times PGE_2 = K_{in} \times \text{stimul}_{\text{PLACEBO}} - K_{out} \times PGE_2 \quad (\text{Eq. 7})$$

$$300 \quad \frac{dPGE_2}{dt} = K_{in} \times \text{stimul}_{\text{NSAIDS}} \times \left[1 - \frac{C_e(t)^n}{IC_{50}^n + C_e(t)^n} \right] - K_{out} \cdot PGE_2 \quad (\text{Eq. 8})$$

301 The time-courses of exudate PGE_2 were modelled simultaneously for placebo and robenacoxib,
 302 then placebo and S(+) ketoprofen, as the equations for placebo and NSAIDs share several
 303 common parameters in the same cat (K_{in} , K_{out} and *carrag*, k_1 and k_2). Nine parameters were
 304 estimated by the model, namely k_{in} , *carrag*, k_1 , k_2 , *tlag1*, *tlag2*, k_{out} , IC_{50} and n .

305

306 *Ex vivo* generation of serum TxB_2 was used as a surrogate marker of COX-1 activity for PK/PD
 307 modelling. The NSAID concentration in the central compartment produced an inhibition of

308 serum TxB₂ synthesis according to the following sigmoid I_{max} model selected to fit the serum
309 TxB₂ data (Eq.9):

$$310 \quad I(C(t)) = I_0(t) - \frac{(I_0 - I_{\max}) \times C(t)^n}{IC_{50}^n + C(t)^n} \quad (\text{Eq. 9})$$

311 where I₀(t) is the baseline serum TxB₂ concentration (ng/mL) for an individual cat, I_{max} (%) is the
312 percentage of maximal TxB₂ suppression (corresponding to the lower limit of quantification of
313 the assay) relative to I₀(t), IC₅₀ (ng/mL) is the concentration that achieves half of the maximal
314 TxB₂ suppression and n is the slope of the NSAID concentration-effect curve. In most cats, the
315 serum TxB₂ concentration had drifted below baseline by the end of the period when placebo was
316 administered, as also reported in a previous study (Pelligand *et al.*, 2012b). This drift of baseline
317 throughout the course of the experiment was modelled as (Eq. 10):

$$318 \quad I_0(t) = I_0 - d \times t \quad (\text{Eq. 10})$$

319 where d represents the slope of the baseline function for an individual cat and I₀ the initial TxB₂
320 concentration during the treatment period (Ollerstam *et al.*, 2006). The slope was calculated for
321 each cat by linear regression of the serum TxB₂ concentration after placebo administration. As
322 blood samples were collected for 48 h during the ketoprofen period but only for 24 h after
323 placebo and robenacoxib dosing, the drift was not applied between 24 h and 48 h (Eq. 11):

$$324 \quad I_0(t \geq 24h) = I_0 - d \times 24 \quad (\text{Eq. 11})$$

325

326 *Calculation of potency indices and estimation of extent of COX-2 blockade centrally*

327 Individual concentration-effect curves for (i) *in vivo* inhibition of COX-2 and (ii) *ex vivo*
328 inhibition of COX-1 were simulated using calculated pharmacodynamic parameters expressing
329 the maximal effect (I_{max}), potency (IC₅₀) and steepness of the NSAIDs concentration-effect

330 relationship (n). An average curve for COX-1 and COX-2 was fitted to the individual curves
331 previously simulated (naïve pooled approach) using the same Hill equation (Giraudel *et al.*,
332 2005b; Pelligand *et al.*, 2012b). The corresponding average parameter values (aIC_{50} and a_n) and
333 95% confidence intervals were derived to calculate the selectivity indices to describe the relative
334 *in vivo* selectivity.. Finally, the predicted percentage of COX-1 inhibition was calculated for 50,
335 80, 95 and 99% inhibition of COX-2.

336

337 *Statistical analysis*

338 Figures and potency curve fitting were computed using Prism version 5 (GraphPad, La Jolla,
339 CA, USA). Statistics were performed with PASW Statistics (version 17, IBM, New York, USA)
340 using a linear mixed model for PGE₂ and TxB₂. Treatment, time and treatment-time interaction
341 were entered as fixed effects and cat was entered as a random effect. Time was nested within
342 treatment and cat, a first order autoregressive covariance structure (AR1) was used (Littell *et al.*,
343 1998; Kristensen & Hansen, 2004). The normality assumption of the residuals was assessed by
344 visual inspection and was verified after a log transformation of exudate PGE₂ and serum TxB₂
345 concentrations. All reported P values are two-tailed, with statistical significance defined as P
346 <0.05. In the *post hoc* tests, multiple analyses were corrected using the Bonferroni method.
347 Arithmetic, geometric and harmonic means are presented (in tables only) as mean \pm SD, mean
348 [95% Confidence Interval] and mean \pm pseudoSD (obtained by the Jackknife method),
349 respectively (Lam *et al.*, 1985).

350

351

352 RESULTS

353 *Pharmacokinetics*

354 Pharmacokinetic parameters for plasma ketoprofen and blood robenacoxib concentrations are
355 summarised in Table 1. The plasma concentration-time curve of ketoprofen was best described
356 by a bicompartamental model with first order absorption for the S(+) enantiomer and a
357 monocompartamental model with first order absorption for the R(-) enantiomer (Fig. 2). Peak
358 plasma concentrations were 4,306 ng/mL for S(+) ketoprofen ($T_{max}= 0.53$ h) and 3,787 ng/mL
359 for R(-) ketoprofen ($T_{max}= 0.25$ h). Apparent clearances (CL/F) were 0.114 L/kg/h for S(+)
360 ketoprofen and 0.325 L/kg/h for R(-) ketoprofen. Terminal elimination half-life was longer for
361 S(+) ketoprofen ($t_{1/2}=1.62$ h, MRT=1.7 h) than for R(-) ketoprofen ($t_{1/2}=0.44$ h, MRT=0.7 h).

362

363 The blood concentration-time curve of robenacoxib was best described by a bicompartamental
364 model with first order absorption (Fig. 3). Peak plasma concentration of 1,313 ng/mL was
365 reached after 0.9 h and the mean absorption t_{lag} was 0.05 h. Apparent blood robenacoxib
366 clearance was moderate (0.684 L/kg/h) (Toutain & Bousquet-Melou, 2004) and elimination half-
367 life was 1.13 h.

368

369 Pharmacokinetic parameters for exudate are summarised in Table 2. The exudate ketoprofen
370 enantiomer concentrations followed a bi-exponential decay (Fig. 2). Harmonic mean penetration
371 half-lives of S(+) and R(-) ketoprofen in exudate were 2.93 h and 2.06 h, respectively. Maximum
372 exudate concentrations were reached at 7.9 h and 6.0 h after injection for S(+) and R(-)
373 ketoprofen, respectively. The mean peak exudate concentration of S(+) ketoprofen was 169
374 ng/mL, and that of R(-) ketoprofen was 44 ng/mL. Elimination half-lives from tissue cages were

375 25.9 h for S(+) and 22.5 h for R(-) ketoprofen, accounting for correspondingly long MRTs of
376 35.9 h and 36.2 h.

377
378 Exudate robenacoxib concentration followed a bi-exponential decay (Fig. 3 and 4). One cat (D2)
379 had peak robenacoxib exudate concentration (351 ng/mL) that was approximately 4-fold higher
380 than the average C_{max} value observed in the other seven cats. However, its exudate
381 concentrations were similar to those observed in the other seven cats by the 12th hour postdose.
382 Since a similar inconsistency was not observed when this cat was administered ketoprofen and
383 because this cat did not behave as an outlier during the pharmacodynamics or blood level PK
384 component of this investigation, it was assumed that these high initial robenacoxib
385 concentrations were a function of experimental error. Accordingly, cat D2 was excluded from
386 the robenacoxib exudate evaluations. However, it should be noted that in the absence of a
387 confirmed source of this error, it is impossible to exclude the possibility that the exudate profiles
388 associated with cat D2 reflect an idiosyncrasy that may exist in a subpopulation of cats. That
389 said, the maximal robenacoxib concentration for the seven other cats was 85.2 ng/mL, attained at
390 8.1 h after dosing. Harmonic mean penetration half-life of robenacoxib in inflammatory exudate
391 was 4.9 h. Exudate elimination half-life and MRT were 41.5 h and 45.7 h, respectively.

392

393

394 Pharmacodynamics

395 Both ketoprofen and robenacoxib reduced exudate PGE₂ concentrations significantly between 6
396 and 36 h (Fig. 5). Maximum PGE₂ inhibition, at 9 h, was 92.1% for robenacoxib and 90.9% for
397 ketoprofen.

398

399 Maximal TxB₂ suppression with robenacoxib was 51.2 % at 2 h and this was the only time when
400 the effect of robenacoxib was significantly different from placebo (Fig. 6). TxB₂ had returned to
401 placebo level at 3 h. With ketoprofen, serum TxB₂ inhibition occurred rapidly, commencing 4
402 min after injection (97.1%) and suppression was maximal (97.9%) at 1 h (Fig. 6). Compared to
403 placebo, ketoprofen significantly suppressed serum TxB₂ between 4 min and 24 h. Serum TxB₂
404 was 11.8% and 58.2% of the placebo concentration at 24 and 48 h, respectively.

405

406

407 *PK/PD analysis*

408 For COX-2 inhibition, the PK/PD model for estimation of pharmacodynamic parameters gave
409 good results in 6 of 8 cats for both S(+) ketoprofen and robenacoxib. In two cats, the model did
410 not converge, because exudate PGE₂ concentrations were reduced below the limit of
411 quantification of the assay or did not recover to the levels in the placebo group within 120 h.
412 Means of individual estimates of the pharmacodynamic COX-2 parameters for the carrageenan
413 model, and after administration of ketoprofen and robenacoxib, are presented in Table 3. The
414 geometric mean COX-2 IC₅₀ was 44.7 ng/mL (0.14 μM) for robenacoxib and 45.0 ng/mL (0.18
415 μM) for S(+) ketoprofen.

416

417 PK/PD modelling for COX-1 was successful in all animals with robenacoxib and in 6 of 8 cats
418 with S(+) ketoprofen. For the latter, in two cases, the number of blood samples was too low to
419 allow bi-compartmental fitting of plasma concentrations and thus prevented PK/PD modelling.
420 Individual geometric mean IC₅₀COX-1 was 2,951 ng/mL (1.31 μM) for robenacoxib and 0.17

421 ng/mL (0.67 nM) for S(+) ketoprofen (Table 4). I_{max} was 97.3 % for S(+) ketoprofen and 96.8 %
422 for robenacoxib.

423

424 Individual concentration-effect curves were simulated using the pharmacodynamic parameters
425 aforementioned. Average pharmacodynamic parameters (aI_{max} , aIC_{50} and a_n) for S(+) ketoprofen
426 and robenacoxib for inhibition of COX-1 in serum and COX-2 in exudate were calculated by
427 naïve pooled data analysis (Table 5 and Fig. 7). The concentration-effect curves for COX-1
428 required re-scaling to a maximal effect of 100%. The aIC_{50} values for COX-1 were 0.45 and 2,56
429 ng/mL for S(+) ketoprofen and robenacoxib and the slopes (a_n) were 0.66 and 0.87, respectively.
430 Corresponding aIC_{50} values for COX-2 were 48.5 and 38.2 ng/mL for S(+) ketoprofen and
431 robenacoxib, respectively, and corresponding slopes were 1.04 and 1.46.

432

433 Three categories of indices were used to describe the selectivity of robenacoxib, determined by
434 simultaneous fitting of individual percentage inhibition values from COX-1 and COX-2 assays
435 (Table 6). The $IC_{50}COX-1/IC_{50}COX-2$ ratio was 1:107 for S(+) ketoprofen and 66.9:1 for
436 robenacoxib. The selectivity of robenacoxib for COX-2 was confirmed at virtually maximal
437 inhibition, as $IC_{99}COX-1/IC_{99}COX-2$ was 585:1. The $IC_{20}COX-1/IC_{80}COX-2$ ratio was 1:3,260
438 for S(+) ketoprofen and 1.4:1 for robenacoxib. Predicted percentage inhibitions of COX-1 versus
439 COX-2 are illustrated in Fig. 8; the inhibition of COX-1 by S(+) ketoprofen would be almost
440 maximal for all COX-2 inhibition percentages between 50 and 99%, whereas only 28.2% of
441 COX-1 activity would be inhibited by robenacoxib at 99% COX-2 inhibition.

442

443

444 DISCUSSION

445

446 S(+) ketoprofen was the predominant enantiomer in the cat, as previously reported for the dog,
447 rat and horse (Foster & Jamali, 1988; Delatour *et al.*, 1993; Landoni & Lees, 1995a). Chiral
448 inversion of R(-) to S(+) ketoprofen occurs in the liver, so that the R(-) enantiomer, although
449 itself of very low potency, is a pro-drug. Therefore, the apparent clearance of R(-) ketoprofen
450 incorporates both elimination and inversion to the S(+) enantiomer. Consequently, the drug input
451 for S(+) ketoprofen comprises both the administered drug and S(+) ketoprofen formed by chiral
452 inversion. The inversion rate has been calculated in the cat by separate administration of each
453 enantiomer (Castro *et al.*, 2000; Lees *et al.*, 2003). Simultaneous enantiomer pharmacokinetic
454 modelling was not possible, as the inversion rate could not be identified from the data of the
455 present study. This study confirmed the short half-life of both ketoprofen enantiomers in the cat.
456 The pharmacokinetics of robenacoxib after subcutaneous administration was also consistent with
457 the findings from previous studies (Pelligand *et al.*, 2012b; King *et al.*, 2013), with a short
458 elimination half-life (1.1 h).

459

460 Despite having short elimination half-lives in blood, ketoprofen and robenacoxib demonstrated
461 marked negative hysteresis. Both drugs suppressed exudate PGE₂ significantly for up to 36 h.
462 The likely explanation is accumulation of drugs in and slow clearance from the tissue cage. It
463 would have been relevant to test this hypothesis by directly injecting the test article into the
464 tissue cages. The IC₅₀ COX-2 for robenacoxib was somewhat higher at 38.2 ng/mL (0.117 μM)
465 in the present study compared with 14.1 ng/mL (0.043 μM) reported in Pelligand *et al.* (2012b).
466 For COX-1, the difference for robenacoxib between the two studies was minimal, with IC₅₀

467 COX-1 of 2,557 ng/mL (7.81 μ M) in the present study and 2,416 ng/mL (7.38 μ M) in the
468 previous investigation.

469

470 The persistence and duration of effect in exudate of ketoprofen enantiomers were similarly long
471 as for robenacoxib. For 2-arylpropionates in general, and for ketoprofen in particular, COX
472 inhibition activity resides almost exclusively with the S(+) enantiomer (Hayball *et al.*, 1992;
473 Suesa *et al.*, 1993; Landoni *et al.*, 1996) in several species including the cat. It is, indeed,
474 probable that COX inhibition in the cat after R(-) ketoprofen administration is attributable solely
475 to the S(+) enantiomer formed *in vivo* by chiral inversion (Lees *et al.*, 2003). It was therefore
476 justified, in this study, to conduct PK/PD modelling solely on S(+) ketoprofen concentration.

477

478 The IC₅₀ COX-2 for S(+) ketoprofen of 48.5 ng/mL (0.191 μ M) was very similar to the IC₅₀ for
479 robenacoxib in the present study (38.2 ng/mL) but was lower than the IC₅₀ reported by Schmid *et*
480 *al.* (2010) in *in vitro* whole blood assays: 119.9 ng/mL (0.472 μ M). In serum, the *ex vivo* IC₅₀ for
481 COX-1 in the present study was 0.454 ng/mL (0.0018 μ M) which was lower than the IC₅₀ of
482 5.92 ng/mL (0.023 μ M) reported by Schmid *et al.* (2010) in *in vitro* assays. Inter-laboratory
483 differences in experimental methodology (*ex vivo* versus *in vitro*) and differences in modelling
484 techniques are well recognised as the basis for differing results, even of this relatively high
485 magnitude (Warner *et al.*, 1999). In consequence, we report an IC₅₀ COX-1 / IC₅₀ COX-2 ratio of
486 1:107, which is lower than that obtained by Schmid *et al.* of 1:20. Despite these numerical
487 differences, both studies confirm that ketoprofen is COX-1 selective in the cat. The time-course
488 of inhibition of TxB₂ with ketoprofen was similar to that reported after intravenous
489 administration of 2 mg/kg racemic ketoprofen (Lees *et al.*, 2003).

490

491 The present data indicate that ketoprofen and robenacoxib exhibit similar pattern for distribution
492 to a site of acute inflammation, whilst possessing opposite selectivities for inhibition of COX
493 isoforms, ketoprofen for COX-1 and robenacoxib for COX-2. As discussed by (Brune & Furst,
494 2007), the first generation selective COX-2 inhibitors (sulphonamides and methylsulphones)
495 combined reduced gastrointestinal toxicity with prolonged inhibition of constitutively-expressed
496 COX-2 in the vascular wall and kidney. This may explain, at least partially, the reported
497 toxicities of these COXibs with long terminal half-lives and large volumes of distribution. It is
498 therefore likely that tissue selectivity is a potential advantage of second generation COXibs
499 (carboxylic acids) with shorter elimination half-lives. If these drugs exert only a short duration of
500 action on constitutively expressed COX-2 in the central pharmacokinetic compartment, this
501 might provide a higher safety profile, for example for cardiovascular and renal side-effects. As
502 developed in our laboratory, the tissue cage model has allowed investigation of the distribution
503 of robenacoxib and ketoprofen (selected for this study for both their differing COX inhibition
504 profiles and long durations of action despite short half-lives in the central pharmacokinetic
505 compartment) to a site of acute inflammation. It may be regarded as an appropriate model to
506 further our understanding of other carboxylic acid NSAIDs, with similar chemical structures and
507 pharmacokinetic profiles, such as lumiracoxib (COX-2 selective) and diclofenac (COX non-
508 selective) (Fig. 8) (Brune & Furst, 2007).

509

510 It should, however, be noted that all tissue cage models are “model dependent”, in that drug
511 diffusion into and from exudate in the cage is influenced by tissue cage geometry (including
512 surface area), a lack of physiological drainage as for the synovial fluid lymph drainage, as well

513 as drug molecule properties, including protein binding, pKa and lipid solubility. Therefore, tissue
514 cage models cannot mimic either accurately or quantitatively all clinical circumstances.
515 Nevertheless, it is of interest to note that lumiracoxib accumulated in inflamed joints in humans
516 and its concentration was maintained in excess of plasma concentrations for up to 18 h after
517 dosing (Scott *et al.*, 2004). Similarly, ketoprofen penetrated readily into acutely inflamed joints
518 of the horse. At one h after dosing the concentration in synovial fluid was six times higher in
519 inflamed compared to non-inflamed joints (Owens *et al.*, 1994). On the other hand,
520 concentrations of etoricoxib (a coxib of the sulphonamide group) in wound fluids did not exceed
521 plasma concentrations after pre-emptive administration before hip surgery (Renner *et al.*, 2010;
522 Renner *et al.*, 2012).

523

524 It is unlikely that the slow clearance of ketoprofen and robenacoxib from tissue cages was
525 limited by passive diffusion. This is suggested by serum and exudate clearance data. For
526 creatinine, an endogenous, non-protein bound small molecule, a $MRT_{\text{exudate}}/MRT_{\text{serum}}$ ratio of
527 3.6:1 was obtained by Pelligand *et al.* (2012a). In contrast, robenacoxib and S(+) ketoprofen
528 $MRT_{\text{exudate}}/MRT_{\text{blood}}$ ratios in the present study were substantially higher, 24.9:1 and 20.4:1
529 respectively. These high ratios are explained by two factors, slow drug clearance from the tissue
530 cages and short half-lives in plasma. Despite the use of tissue cages of different geometry
531 (spherical polypropylene cages instead of silicon cylinders similar to the feline tissue cages),
532 previous workers showed that the ketoprofen MRT ratio was also high (11.5:1) in the goat
533 (Arifah *et al.*, 2003) and in the calf (10.6:1) (Landoni & Lees, 1995b) though not in the horse
534 (2.9:1). Moreover, other tissue cage investigations demonstrated that not all COXibs are tissue

535 selective; the $MRT_{\text{exudate}}/MRT_{\text{blood}}$ ratio for firocoxib in the dog (a methylsulphone related to
536 rofecoxib) was 1.06:1 and similar to meloxicam 1.08:1 (P. Lees, unpublished data).

537
538 The binding of drugs to and slow release from a component of the inflammatory process, such as
539 protein or a specific cell population, could account for these differing results for NSAIDs
540 (Pelligand *et al.*, 2012b). For example, the search for the ideal radiolabelled marker for imaging
541 COX-2 expression revealed that a radioiodinated derivative of lumiracoxib had a higher affinity
542 and *in vitro* cell uptake for COX-2 induced macrophages than normal macrophages (Kuge *et al.*,
543 2009). A similar mechanism might explain the slow clearance of robenacoxib from exudate.

544 The prolonged plasma half-life of the sulphonamide COXibs (celecoxib, etoricoxib and
545 valdecoxib) is explained both by slow clearance and relatively high volume of distribution. In
546 contrast, the volume of distribution of carboxylic acid COXibs is very small compared to other
547 classes of COXibs. Thus, lumiracoxib steady state volume of distribution was 9 L in humans
548 (0.13L/kg for a 70kg person, Mysler, 2004) and the distribution volume for robenacoxib was
549 likewise low, 0.19 L/kg in the cat and 0.24 L/kg in the dog (Jung *et al.*, 2009; Pelligand *et al.*,
550 2012b).

551
552 The sulphonamide moiety of a radioiodinated derivative of celecoxib had a high affinity for
553 carbonic anhydrase and this could explain both the preferential distribution into rat erythrocytes
554 (88%) and slow clearance from blood (Boddy *et al.*, 1989; Kuge *et al.*, 2006). Substitution of the
555 sulphonamide moiety to a methylsulphone moiety decreased erythrocyte binding to 18% and
556 increased blood clearance (Kuge *et al.*, 2006).

557

558 In conclusion, the present data suggest that, despite a short blood half-life, NSAIDs can have a
559 long-lasting local action, as a consequence of high inflammatory tissue selectivity. However,
560 drug distribution into tissue cage fluid is model dependant and cannot be a precise predictor of
561 penetration time course to other anatomical sites. This will indeed depend on a wide range of
562 factors, including specific tissue blood flow and possibly the degree of acute inflammation.
563 Tissue selectivity might be advantageous for carboxylic acids COXibs and some older NSAIDs
564 such as ketoprofen and diclofenac, as systemic side-effects related to COX-1 and COX-2
565 inhibition could be reduced, whilst efficacy in experimental inflammation persists for 24 h or
566 longer after a single dose.

567

568

569 ACKNOWLEDGEMENTS

570 This study was supported by Novartis Animal Health, Inc and the Biotechnology and Biological
571 Sciences Research Council UK (Industrial CASE Award) [grant number: BB/E528544/1]
572 awarded to L.P. We thank Birgit Ranheim for initiating the collaboration with the Oslo School of
573 Veterinary Science.

574

575 DECLARATIONS OF INTEREST

576 L. Pelligand received a CASE award from BBSRC and Novartis Animal Health

577 J.N. King is an employee of Novartis Animal Health

578 P. Lees has acted as a consultant to Novartis Animal Health

579

580 REFERENCES

- 582 Arifah, A.K., Landoni, M.F. & Lees, P. (2003) Pharmacodynamics, chiral pharmacokinetics and
583 PK-PD modelling of ketoprofen in the goat. *Journal of Veterinary Pharmacology and*
584 *Therapeutics*, **26**(2), 139-150.
- 585 Boddy, A., Edwards, P. & Rowland, M. (1989) Binding of sulfonamides to carbonic anhydrase:
586 influence on distribution within blood and on pharmacokinetics. *Pharm Res*, **6**(3), 203-
587 209.
- 588 Bombardier, C., Laine, L., Reicin, A., Shapiro, D., Burgos-Vargas, R., Davis, B., Day, R.,
589 Ferraz, M.B., Hawkey, C.J., Hochberg, M.C., Kvien, T.K. & Schnitzer, T.J. (2000)
590 Comparison of upper gastrointestinal toxicity of rofecoxib and naproxen in patients with
591 rheumatoid arthritis. VIGOR Study Group. *New England Journal of Medicine*, **343**(21),
592 1520-1528.
- 593 Brune, K. & Furst, D.E. (2007) Combining enzyme specificity and tissue selectivity of
594 cyclooxygenase inhibitors: towards better tolerability? *Rheumatology (Oxford)*, **46**(6),
595 911-919.
- 596 Castro, E., Soraci, A., Fogel, F. & Tapia, O. (2000) Chiral inversion of R(-) fenoprofen and
597 ketoprofen enantiomers in cats. *Journal of Veterinary Pharmacology and Therapeutics*,
598 **23**(5), 265-271.
- 599 Dayneka, N.L., Garg, V. & Jusko, W.J. (1993) Comparison of four basic models of indirect
600 pharmacodynamic responses. *Journal of pharmacokinetics and biopharmaceutics*, **21**(4),
601 457-478.
- 602 Delatour, P., Benoit, E., Bourdin, M., Gobron, M. & Moysan, F. (1993) [Comparative
603 enantioselectivity of the disposition of two non-steroidal anti-inflammatory agents,
604 ketoprofen and carprofen, in man and animals]. *Bulletin de l'Académie nationale de*
605 *médecine.*, **177**(3), 515-526.
- 606 Farkouh, M.E., Kirshner, H., Harrington, R.A., Ruland, S., Verheugt, F.W., Schnitzer, T.J.,
607 Burmester, G.R., Mysler, E., Hochberg, M.C., Doherty, M., Ehram, E., Gitton, X.,
608 Krammer, G., Mellein, B., Gimona, A., Matchaba, P., Hawkey, C.J. & Chesebro, J.H.
609 (2004) Comparison of lumiracoxib with naproxen and ibuprofen in the Therapeutic
610 Arthritis Research and Gastrointestinal Event Trial (TARGET), cardiovascular outcomes:
611 randomised controlled trial. *Lancet*, **364**(9435), 675-684.
- 612 Fosse, T.K., Horsberg, T.E., Haga, H.A., Hormazabal, V. & Ranheim, B. (2011)
613 Enantioselective pharmacokinetics of ketoprofen in piglets: the significance of neonatal
614 age. *Journal of Veterinary Pharmacology and Therapeutics*, **34**(2), 153-159.
- 615 Foster, R.T. & Jamali, F. (1988) Stereoselective pharmacokinetics of ketoprofen in the rat.
616 Influence of route of administration. *Drug metabolism and disposition*, **16**(4), 623-626.
- 617 Giraudel, J.M., Diquelou, A., Laroute, V., Lees, P. & Toutain, P.L. (2005a)
618 Pharmacokinetic/pharmacodynamic modelling of NSAIDs in a model of reversible
619 inflammation in the cat. *Br J Pharmacol*, **146**(5), 642-653.
- 620 Giraudel, J.M., Diquelou, A., Lees, P. & Toutain, P.L. (2005b) Development and validation of a
621 new model of inflammation in the cat and selection of surrogate endpoints for testing
622 anti-inflammatory drugs. *J Vet Pharmacol Ther*, **28**(3), 275-285.
- 623 Hayball, P.J., Nation, R.L. & Bochner, F. (1992) Enantioselective pharmacodynamics of the
624 nonsteroidal antiinflammatory drug ketoprofen: in vitro inhibition of human platelet
625 cyclooxygenase activity. *Chirality*, **4**(8), 484-487.

- 626 Higgins, A.J. & Lees, P. (1984) Arachidonic acid metabolites in carrageenin-induced equine
627 inflammatory exudate. *Journal of Veterinary Pharmacology and Therapeutics*, **7**(1), 65-
628 72.
- 629 Jung, M., Lees, P., Seewald, W. & King, J.N. (2009) Analytical determination and
630 pharmacokinetics of robenacoxib in the dog. *Journal of Veterinary Pharmacology and*
631 *Therapeutics*, **32**(1), 41-48.
- 632 Kamata, M., King, J.N., Seewald, W., Sakakibara, N., Yamashita, K. & Nishimura, R. (2012)
633 Comparison of injectable robenacoxib versus meloxicam for peri-operative use in cats:
634 Results of a randomised clinical trial. *The Veterinary Journal*, **193**(1), 114-118.
- 635 Kelley, M. & DeSilva, B. (2007) Key elements of bioanalytical method validation for
636 macromolecules. *The AAPS journal*, **9**(2), E156-163.
- 637 King, J.N., Jung, M., Maurer, M.P., Seewald, W., Schmid, V. & Lees, P. (2013) Effects of route
638 of administration and feeding schedule on pharmacokinetics of robenacoxib in cats. *Am J*
639 *Vet Res*, **74**(3), 465-472.
- 640 Kristensen, M. & Hansen, T. (2004) Statistical analyses of repeated measures in physiological
641 research: a tutorial. *Adv Physiol Educ*, **28**(1-4), 2-14.
- 642 Kuge, Y., Katada, Y., Shimonaka, S., Temma, T., Kimura, H., Kiyono, Y., Yokota, C.,
643 Minematsu, K., Seki, K., Tamaki, N., Ohkura, K. & Saji, H. (2006) Synthesis and
644 evaluation of radioiodinated cyclooxygenase-2 inhibitors as potential SPECT tracers for
645 cyclooxygenase-2 expression. *Nucl Med Biol*, **33**(1), 21-27.
- 646 Kuge, Y., Obokata, N., Kimura, H., Katada, Y., Temma, T., Sugimoto, Y., Aita, K., Seki, K.,
647 Tamaki, N. & Saji, H. (2009) Synthesis and evaluation of a radioiodinated lumiracoxib
648 derivative for the imaging of cyclooxygenase-2 expression. *Nucl Med Biol*, **36**(8), 869-
649 876.
- 650 Lam, F.C., Hung, C.T. & Perrier, D.G. (1985) Estimation of variance for harmonic mean half-
651 lives. *J Pharm Sci*, **74**(2), 229-231.
- 652 Landoni, M.F., Foot, R., Frean, S. & Lees, P. (1996) Effects of flunixin, tolfenamic acid, R(-)
653 and S(+) ketoprofen on the response of equine synoviocytes to lipopolysaccharide
654 stimulation. *Equine veterinary journal*, **28**(6), 468-475.
- 655 Landoni, M.F. & Lees, P. (1995a) Comparison of the anti-inflammatory actions of flunixin and
656 ketoprofen in horses applying PK/PD modelling. *Equine veterinary journal*, **27**(4), 247-
657 256.
- 658 Landoni, M.F. & Lees, P. (1995b) Pharmacokinetics and pharmacodynamics of ketoprofen
659 enantiomers in calves. *Chirality*, **7**(8), 586-597.
- 660 Lees, P., Giraudel, J., Landoni, M.F. & Toutain, P.L. (2004) PK-PD integration and PK-PD
661 modelling of nonsteroidal anti-inflammatory drugs: principles and applications in
662 veterinary pharmacology. *Journal of Veterinary Pharmacology and Therapeutics*, **27**(6),
663 491-502.
- 664 Lees, P., Taylor, P.M., Landoni, F.M., Arifah, A.K. & Waters, C. (2003) Ketoprofen in the cat:
665 pharmacodynamics and chiral pharmacokinetics. *The Veterinary Journal*, **165**(1), 21-35.
- 666 Lepist, E.I. & Jusko, W.J. (2004) Modeling and allometric scaling of s(+)-ketoprofen
667 pharmacokinetics and pharmacodynamics: a retrospective analysis. *Journal of Veterinary*
668 *Pharmacology and Therapeutics*, **27**(4), 211-218.
- 669 Littell, R.C., Henry, P.R. & Ammerman, C.B. (1998) Statistical analysis of repeated measures
670 data using SAS procedures. *J Anim Sci*, **76**(4), 1216-1231.

- 671 Mysler, E. (2004) Lumiracoxib (Prexige): a new selective COX-2 inhibitor. *Int J Clin Pract*,
672 **58**(6), 606-611.
- 673 Nantel, F., Denis, D., Gordon, R., Northey, A., Cirino, M., Metters, K.M. & Chan, C.C. (1999)
674 Distribution and regulation of cyclooxygenase-2 in carrageenan-induced inflammation.
675 *Br J Pharmacol*, **128**(4), 853-859.
- 676 Ollerstam, A., Visser, S.A., Persson, A.H., Eklund, G., Nilsson, L.B., Forsberg, T., Wiklund,
677 S.J., Gabrielsson, J., Duker, G. & Al-Saffar, A. (2006) Pharmacokinetic-
678 pharmacodynamic modeling of drug-induced effect on the QT interval in conscious
679 telemetered dogs. *Journal of pharmacological and toxicological methods*, **53**(2), 174-
680 183.
- 681 Owens, J.G., Kammerling, S.G. & Keowen, M.L. (1994) Anti-inflammatory effects and
682 pharmacokinetics of ketoprofen in a model of equine synovitis. In Abstract of the 6th
683 EAVPT Congress. *Journal of Veterinary Pharmacology and Therapeutics*, **27**(s1), 170-
684 171.
- 685 Pelligand, L., House, A.K., Summers, B.A., Hatzis, A., Tivers, M., Elliott, J. & Lees, P. (2012a)
686 Development and validation of a tissue cage model of acute inflammation in the cat.
687 *Journal of Veterinary Pharmacology and Therapeutics*, **35**, 239-248.
- 688 Pelligand, L., King, J.N., Toutain, P.L., Elliott, J. & Lees, P. (2012b) PK-PD modelling of
689 robenacoxib in a feline tissue cage model of inflammation. *Journal of Veterinary
690 Pharmacology and Therapeutics*, **35**(1), 19-32.
- 691 Renner, B., Walter, G., Strauss, J., Fromm, M.F., Zacher, J. & Brune, K. (2012) Preoperative
692 administration of etoricoxib in patients undergoing hip replacement causes inhibition of
693 inflammatory mediators and pain relief. *European Journal of Pain*, **16**(6), 838-848.
- 694 Renner, B., Zacher, J., Buvanendran, A., Walter, G., Strauss, J. & Brune, K. (2010) Absorption
695 and distribution of etoricoxib in plasma, CSF, and wound tissue in patients following hip
696 surgery--a pilot study. *Naunyn Schmiedebergs Arch Pharmacol*, **381**(2), 127-136.
- 697 Rudy, A.C., Liu, Y., Brater, C. & Hall, S.D. (1998) Stereoselective pharmacokinetics and
698 inversion of (R)- ketoprofen in healthy volunteers. *J Clin Pharmacol*, **38**(2 Suppl), 3S-
699 10S.
- 700 Schmid, V.B., Seewald, W., Lees, P. & King, J.N. (2010) In vitro and ex vivo inhibition of COX
701 isoforms by robenacoxib in the cat: a comparative study. *Journal of Veterinary
702 Pharmacology and Therapeutics*, **33**(5), 444-452.
- 703 Scott, G., Rordorf, C., Reynolds, C., Kalbag, J., Looby, M., Milosavljev, S., Weaver, M., Huff,
704 J.P. & Ruff, D.A. (2004) Pharmacokinetics of lumiracoxib in plasma and synovial fluid.
705 *Clinical Pharmacokinetics*, **43**(7), 467-478.
- 706 Silverstein, F.E., Faich, G., Goldstein, J.L., Simon, L.S., Pincus, T., Whelton, A., Makuch, R.,
707 Eisen, G., Agrawal, N.M., Stenson, W.F., Burr, A.M., Zhao, W.W., Kent, J.D.,
708 Lefkowitz, J.B., Verburg, K.M. & Geis, G.S. (2000) Gastrointestinal toxicity with
709 celecoxib vs nonsteroidal anti-inflammatory drugs for osteoarthritis and rheumatoid
710 arthritis: the CLASS study: A randomized controlled trial. Celecoxib Long-term Arthritis
711 Safety Study. *Journal of the American Medical Association*, **284**(10), 1247-1255.
- 712 Suesa, N., Fernandez, M.F., Gutierrez, M., Rufat, M.J., Rotllan, E., Calvo, L., Mauleon, D. &
713 Carganico, G. (1993) Stereoselective cyclooxygenase inhibition in cellular models by the
714 enantiomers of ketoprofen. *Chirality*, **5**(8), 589-595.

715 Tomlinson, A., Appleton, I., Moore, A.R., Gilroy, D.W., Willis, D., Mitchell, J.A. &
716 Willoughby, D.A. (1994) Cyclo-oxygenase and nitric oxide synthase isoforms in rat
717 carrageenin-induced pleurisy. *Br J Pharmacol*, **113**(3), 693-698.

718 Toutain, P.L. & Bousquet-Melou, A. (2004) Plasma clearance. *J Vet Pharmacol Ther*, **27**(6),
719 415-425.

720 Vasquez-Bahena, D.A., Salazar-Morales, U.E., Ortiz, M.I., Castaneda-Hernandez, G. &
721 Troconiz, I.F. (2010) Pharmacokinetic-pharmacodynamic modelling of the analgesic
722 effects of lumiracoxib, a selective inhibitor of cyclooxygenase-2, in rats. *Br J Pharmacol*,
723 **159**(1), 176-187.

724 Viswanathan, C.T., Bansal, S., Booth, B., DeStefano, A.J., Rose, M.J., Sailstad, J., Shah, V.P.,
725 Skelly, J.P., Swann, P.G. & Weiner, R. (2007) Quantitative bioanalytical methods
726 validation and implementation: best practices for chromatographic and ligand binding
727 assays. *Pharm Res*, **24**(10), 1962-1973.

728 Wallace, J.L., Chapman, K. & McKnight, W. (1999) Limited anti-inflammatory efficacy of
729 cyclo-oxygenase-2 inhibition in carrageenan-airpouch inflammation. *Br J Pharmacol*,
730 **126**(5), 1200-1204.

731 Warner, T.D., Giuliano, F., Vojnovic, I., Bukasa, A., Mitchell, J.A. & Vane, J.R. (1999)
732 Nonsteroid drug selectivities for cyclo-oxygenase-1 rather than cyclo-oxygenase-2 are
733 associated with human gastrointestinal toxicity: a full in vitro analysis. *Proc Natl Acad
734 Sci U S A*, **96**(13), 7563-7568.

735 Yamaoka, K., Nakagawa, T. & Uno, T. (1978) Application of Akaike's information criterion
736 (AIC) in the evaluation of linear pharmacokinetic equations. *J Pharmacokinet Biopharm*,
737 **6**(2), 165-175.

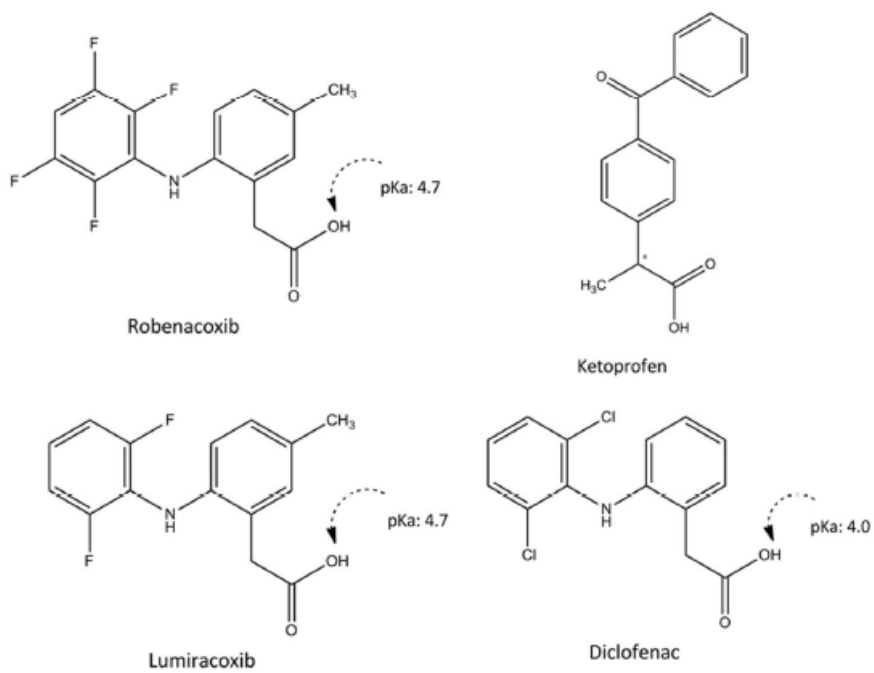
738

739

741 **Figure legends:**

742 Figure 1: Chemical formulae for ketoprofen and diclofenac related COXibs: lumiracoxib and

743 robenacoxib

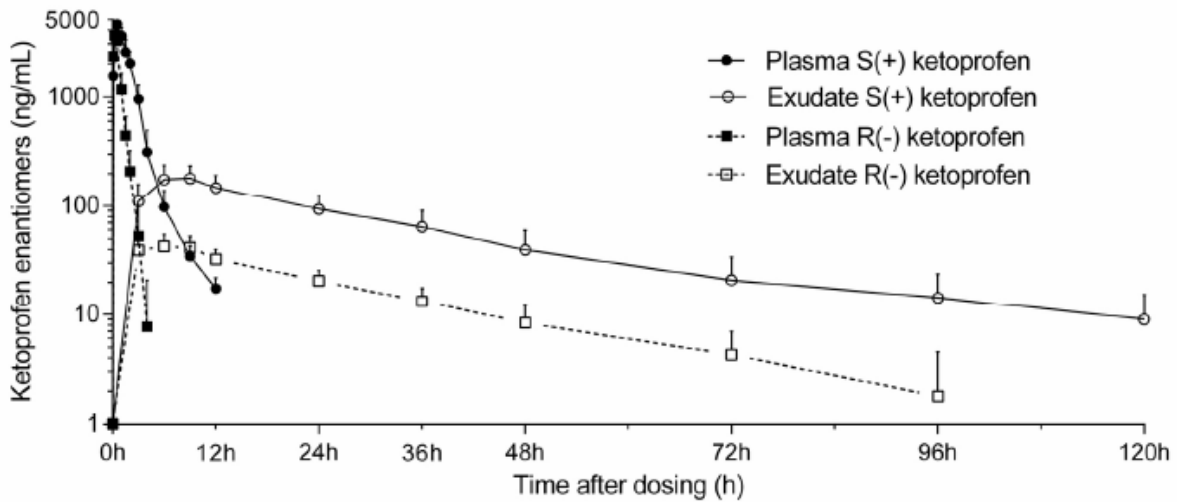


254x190mm (96 x 96 DPI)

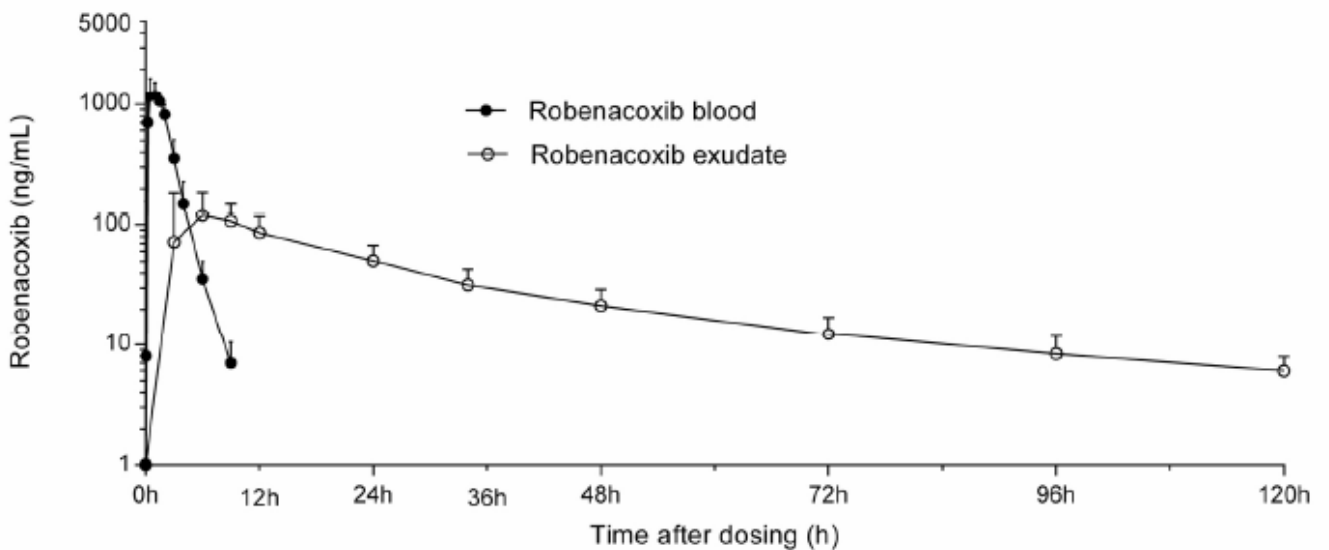
744

745

746 Figure 2: Observed plasma S(+) ketoprofen (●), R(-) ketoprofen (■), exudate S(+) ketoprofen (○)
 747 and exudate R(-) ketoprofen (□) concentrations (ng/mL) versus time (h) profiles after
 748 subcutaneous administration of racemic ketoprofen at a total dose of 2 mg/kg. Results from eight
 749 cats are presented as mean ±SD.

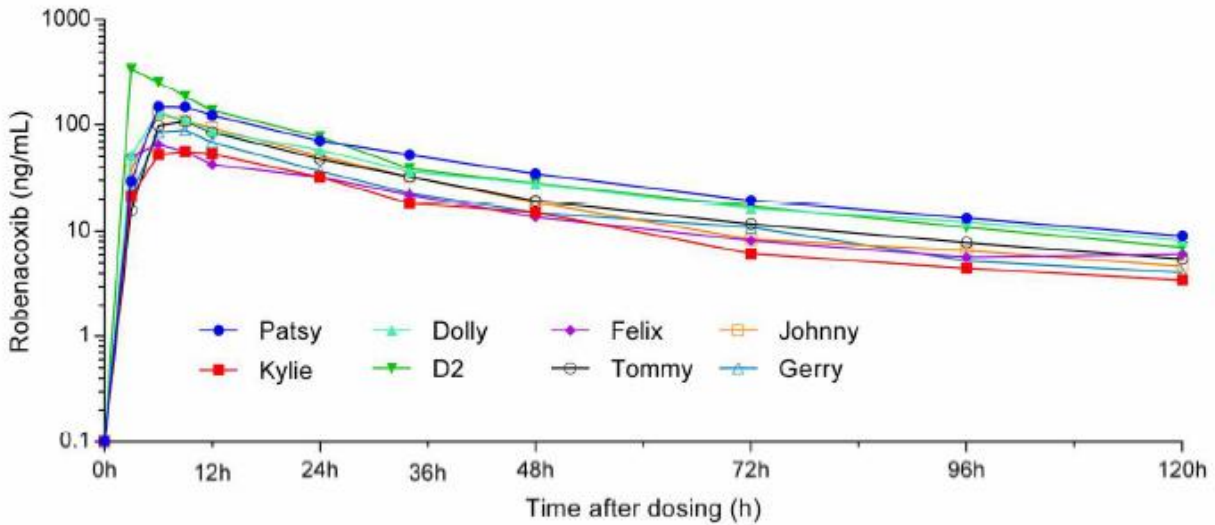


750
 751 Figure 3: Observed blood (●) and exudate (○) robenacoxib concentration (ng/mL) versus time
 752 (h) profiles after subcutaneous administration of a 2 mg/kg dose. Results from 8 cats are
 753 presented as mean +SD.

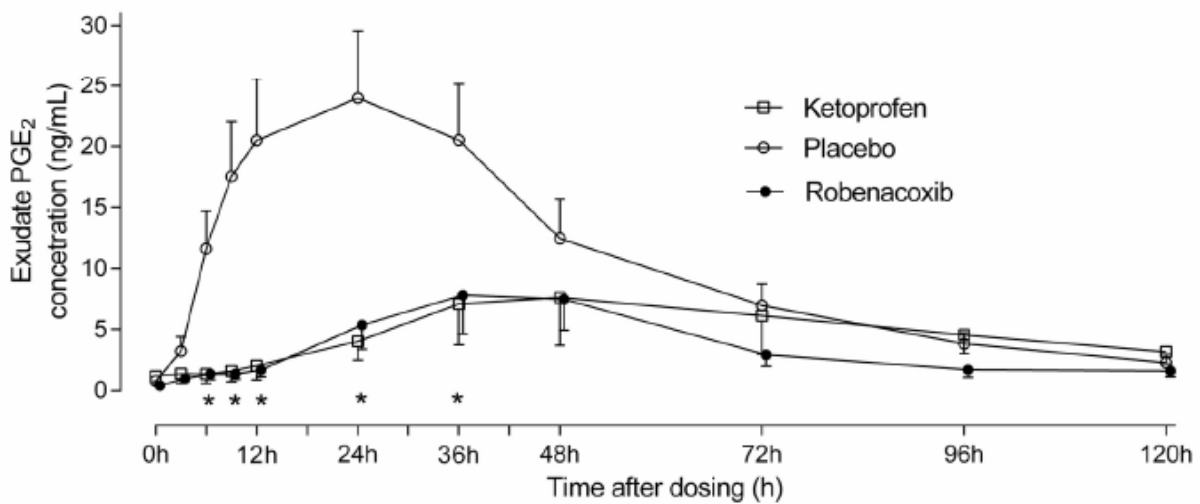


754

755 Figure 4: Individual exudate robenacoxib concentration (ng/mL) versus time (h) profiles after
 756 subcutaneous administration of a 2 mg/kg dose.

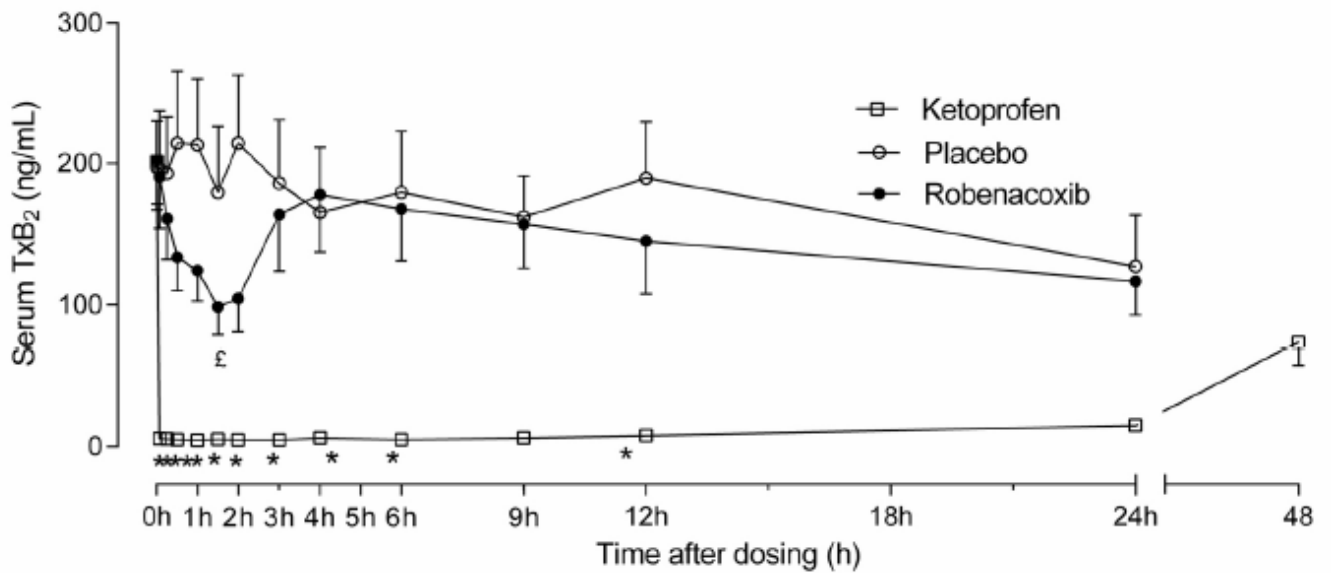


757
 758 Figure 5: Exudate PGE₂ concentration (ng/mL) versus time (h) profiles after carrageenan
 759 injection and placebo, racemic ketoprofen (2mg/kg total dose) and robenacoxib (2 mg/kg)
 760 subcutaneous administration. PK/PD modelling is relevant to the time-response profile as a
 761 whole rather than to the response at sampling times taken separately and therefore values are
 762 presented as mean ±SEM. Statistical comparison of effect of treatment versus placebo (* = P
 763 <0.05) at different times (linear mixed effect model).



764

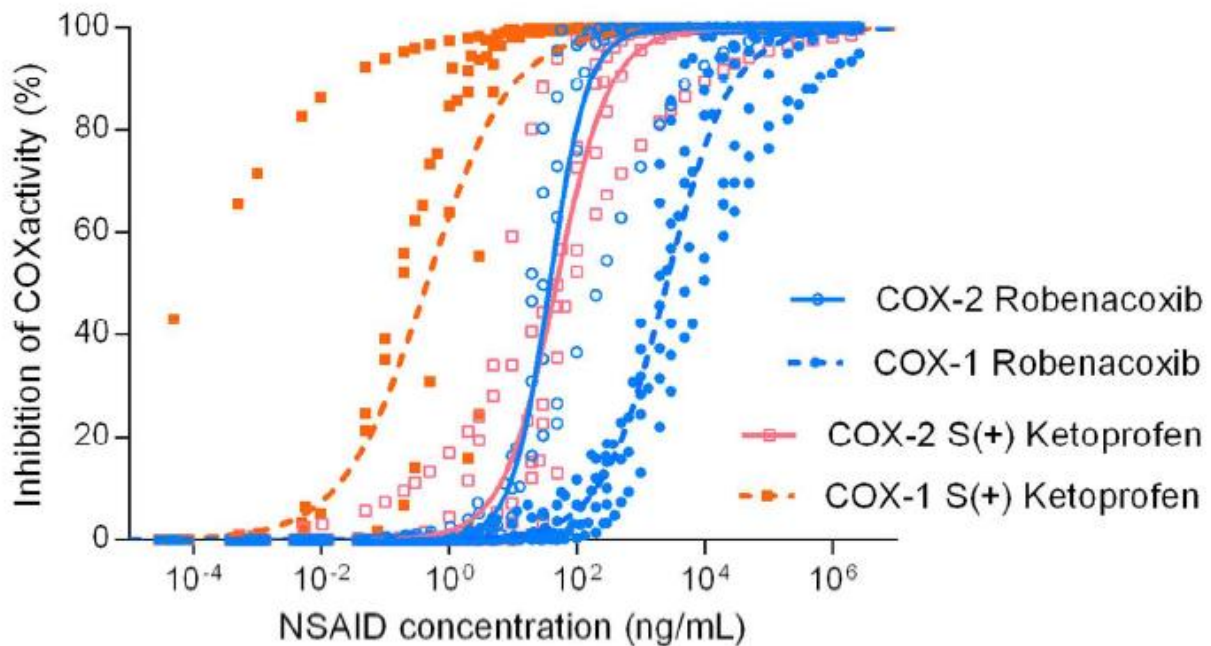
765 Figure 6: Serum TxB₂ concentration (ng/mL) versus time (h) profile after placebo, racemic
 766 ketoprofen (2 mg/kg total dose) and robenacoxib (2 mg/kg) subcutaneous administration. PK/PD
 767 modelling is relevant to the time-response profile as a whole rather than to the response at
 768 sampling times taken separately and therefore values are presented as mean ±SEM. Statistical
 769 comparison of effect of ketoprofen versus placebo (* = P <0.05) and robenacoxib versus placebo
 770 (£ = P <0.05) at different times (linear mixed effect model).



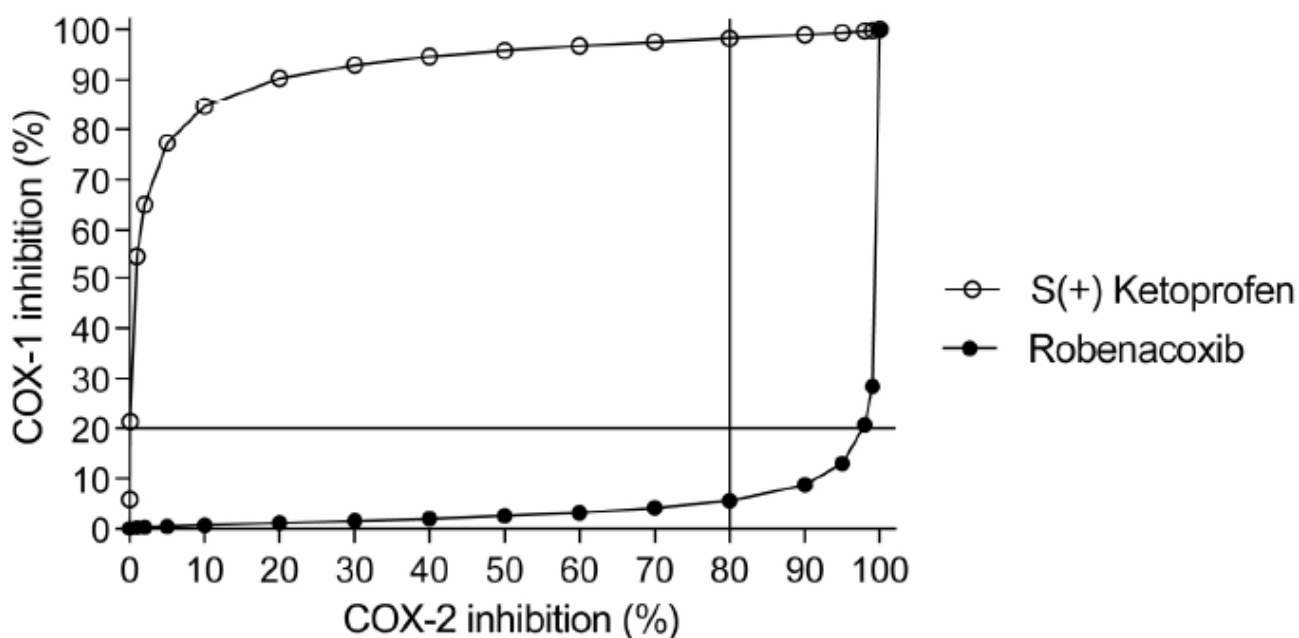
771

772

773 Figure 7: Observed and fitted COX inhibition (%) versus S(+) ketoprofen (red) and robenacoxib
774 (blue) concentrations (ng/mL). Open and closed symbols represent COX-2 and COX-1,
775 respectively. COX-1 data were rescaled for 100% I_{max} . In a naïve pooled data analysis, average
776 regression curves for COX-1 and COX-2 were fitted with a sigmoid I_{max} model to all individual
777 curves (n= 6 to 8 cats for each regression curve).



780 Figure 8: Inhibition percentage of COX-2 and corresponding inhibition percentages of COX-1
781 for a range of concentration of S(+) ketoprofen and robenacoxib. Mean inhibition curves were
782 computed by non-linear regression, fitting an average Hill equation (I_{max} model) to individual
783 concentration-effect profiles (ranging from 0 to I_{max} and rescaled on 0-100% scales), previously
784 obtained by solving PK/PD models for serum TxB_2 inhibition (COX-1 activity) and exudate
785 PGE_2 inhibition (COX-2 activity). Average NSAID concentrations for given inhibition
786 percentages of COX-2 were used to determine corresponding COX-1 inhibition percentage.
787 Dotted lines indicate cut off values for inhibition of COX-1 (above 20% inhibition of COX-1
788 increased risk of side-effects) and COX-2 (above 80% inhibition of COX-2 correlates with good
789 clinical efficacy).



790

791 **Table 1.** Mean pharmacokinetic parameters for plasma S(+) ketoprofen and R(-) ketoprofen and blood robenacoxib concentrations after single
 792 subcutaneous administration of racemic ketoprofen (total nominal dose of 2 mg/kg) or robenacoxib (nominal dose 2 mg/kg) in 8 healthy cats

Parameter	Unit	S(+) Ketoprofen		R(-) Ketoprofen		Robenacoxib	
		Mean*	SD or [95%CI]	Mean*	SD or [95%CI]	Mean*	SD or [95%CI]
T _{max}	h	0.53	0.12	0.25	0.04	0.9	0.24
C _{max}	ng/mL	4,306	[3,566-5,198]	3,787	[3,015-4,757]	1,313	[1,033-1,668]
AUC _{0-inf}	ng.h/mL	8,778	[7,043-10,939]	3,082	[2,338-4,062]	3,043	[2,782-3,329]
MRT	h	1.73	0.27	0.68	0.16	1.85	0.38
t _{1/2}	h	1.62	1.14	0.44	0.19	1.13	0.18
V _{z_F}	L/kg	0.308	[0.192-0.495]	0.222	[0.148-0.331]	1.130	[0.949-1.344]
CL _F	L/h/kg	0.114	[0.092-0.142]	0.325	[0.246-0.428]	0.684	[0.622-0.753]

793 * T_{max} and MRT are presented as arithmetic mean ± SD, half lives presented as harmonic means with pseudo-SD estimated by the jackknife
 794 method. All other parameters are presented as geometric mean [95% CI of the mean], Calculation methods are given in the text. T_{max} : time of
 795 maximal concentration, C_{max} : maximal concentration, AUC_{0-inf} : area under concentration versus time curve extrapolated to infinity, λz slope of
 796 the drug elimination phase and t_{1/2} corresponding elimination half life, V_{z_F} : volume of the central compartment scaled by bioavailability F,
 797 CL_F : body clearance scaled by bioavailability.

798 **Table 2.** Mean pharmacokinetic parameters for exudate S(+) ketoprofen and R(-) ketoprofen and robenacoxib concentrations after single
799 subcutaneous administration of racemic ketoprofen (total nominal dose of 2 mg/kg) or robenacoxib (nominal dose 2 mg/kg) in 8 healthy cats

	Unit	S(+) Ketoprofen		R(-) Ketoprofen		Robenacoxib*	
		Mean	SD or [95%CI]	Mean	SD or [95%CI]	Mean	SD or [95%CI]
T _{max}	h	7.9	2.35	6.0	2.55	8.1	2.79
C _{max}	ng/mL	169.1	[133.5-214.1]	43.9	[34.9-55.2]	85.2	[63.1-115.1]
t _{1/2} K _{ea}	h	2.93	2.29	2.06	1.52	4.86	2.99
MRT	h	35.89	7.41	36.22	14.85	45.68	6.07
t _{1/2}	h	25.88	3.67	22.54	12.29	41.48	8.85

800

801 T_{max} and MRT are presented as arithmetic mean ±SD, half-lives are presented as harmonic mean with pseudo-SD estimated by the jackknife
802 method. All other parameters are presented as geometric mean [95% CI of the mean]. See text for calculation methods. T_{max} is the time of
803 maximal concentration C_{max} is maximum concentration; t_{1/2} K_{ea} and t_{1/2}: half-life of penetration in exudate and elimination from exudate
804 respectively; MRT: mean residence time in exudate calculated by non-compartmental analysis.

805 * One cat had exceptionally high exudate robenacoxib concentration and was not included in the calculations.

806

807 **Table 3.** Individual pharmacodynamic parameters describing the inhibitory effect of
 808 robenacoxib (2 mg/kg) and ketoprofen (2 mg/kg racemate) on exudate PGE₂ production
 809 after subcutaneous administration

Parameter	Unit	Robenacoxib*		Ketoprofen*	
		Mean	95% CI or [range]	Mean	95% CI or [range]
K _{in}	ng/mL/h	0.28	0.01-0.79	0.42	0.10-1.74
Carrag	no unit	33.3	11.0-100.9	10.5	4.6-24.2
k ₁	/h	0.21	0.08-0.54	0.52	0.15-1.83
k ₂	/h	0.05	0.03-0.10	0.03	0.02-0.05
N	no unit	2.0	1.09-3.78	1.39	0.67-2.79
IC ₅₀	ng/mL	44.7	16.9-118.2	45.9	17.8-118.7
K _{out}	/h	0.12	0.04-0.39	0.16	0.09-0.29
t _{lag1} (placebo)	h	0.5	[0-2.9]	2.9	[0.5-7.2]
t _{lag2} (NSAID)	h	5.4	[0-16.5]	9.8	[0-22.0]

810 An indirect response model including 9 estimated parameters was computed.

811 * The results from 2 of 8 cats were excluded from the calculation of the mean because the
 812 inhibition of exudate PGE₂ never recovered below 50% of placebo PGE₂. k₁ and k₂: first
 813 order time dependent variables for growth and dissipation of carrageenan stimulation on
 814 COX (respectively). Carrag is a scalar, K_{in} is a zero-order constant for basal PGE₂
 815 production, K_{out} is a first-order rate constant for removal of PGE₂ from exudate; t_{lag1} and
 816 t_{lag2}: lag time between injection of carrageenan and beginning of the carrageenan
 817 stimulation for the placebo function (t_{lag1}) and for the NSAIDs function (t_{lag2}). Data are
 818 reported as geometric mean with 95% CI of the mean except t_{lags} (arithmetic mean,
 819 [range])

820 **Table 4.** Individual pharmacodynamic parameters describing the inhibitory effect of
 821 robenacoxib (2 mg/kg) and ketoprofen (2 mg/kg racemate) on serum TxB₂ production
 822 (COX-1 activity) after subcutaneous administration.
 823

Parameter	Unit	Robenacoxib		Ketoprofen*	
		Mean	95% CI	Mean	95% CI
I ₀	ng/mL	174	115-262	201	134-301
IC ₅₀	ng/mL	2,951	1,498-5,815	0.168	0.003-9.732
N	no unit	1.01	0.65-1.58	1.67	0.57-4.91

824

825 *The results from two of eight cats receiving ketoprofen were excluded, as the number of
 826 samples was too low to fit a biexponential model to the blood concentration time profile.
 827 Data were fitted using a sigmoid I_{max} model for robenacoxib (8 cats) and ketoprofen (6
 828 cats). I_{max} is the percentage of maximal suppression of TxB₂ (corresponding to the lower
 829 limit of quantification of the assay) relative to I₀(t). I₀ is the fitted value of intercept at
 830 time 0 taking into account baseline drift in TxB₂ concentrations observed after placebo
 831 dosing. Data are presented as geometric mean and 95% CI of the mean for I₀, IC₅₀ and n.
 832

833 **Table 5.** Average maximal effect (aI_{max}), potency (aIC_{50}) and slope (a_n) of S(+)
 834 ketoprofen and robenacoxib for *ex vivo* inhibition of COX-1 in serum and *in vivo*
 835 inhibition of COX-2 in exudate
 836

PD parameters	aI_{max}	aIC_{50}	[95%CI]	a_n	[95%CI]
Units	%	ng/mL		(no unit)	
COX-1					
Ketoprofen	97.3	0.45	[0.32 - 0.65]	0.66	[0.51 - 0.81]
Robenacoxib	96.8	2557	[2291 – 2818]	0.87	[0.80 - 0.94]
COX-2					
Ketoprofen	100.0	48.5	[41.6 - 56.6]	1.04	[0.89 - 1.19]
Robenacoxib	100.0	38.2	[33.9 - 42.7]	1.46	[1.22 - 1.70]

837
 838 Reported parameters and bounds of the 95% confidence interval [95%CI] were calculated
 839 by naïve pooled data analysis (Giraudel *et al.*, 2005). An average curve was fitted with a
 840 sigmoid I_{max} model to all simulated curves (n=8 cats for robenacoxib COX-1 and 6 cats
 841 otherwise) as if they were data from a single individual.
 842

843 **Table 6.** Three categories of indices describing the *in vivo* selectivity of robenacoxib
 844 determined by simultaneous fitting of individual percentage inhibition values from COX-
 845 1 and COX-2 assays

	Ketoprofen	Robenacoxib
Classical selectivity ratios:		
IC ₅₀ / IC ₅₀	1 : 107	66.9 : 1
IC ₈₀ / IC ₈₀	1 : 50.4	129 : 1
IC ₉₅ / IC ₉₅	1 : 21.6	268 : 1
IC ₉₉ / IC ₉₉	1 : 8.8	585 : 1
IC ₂₀ / IC ₈₀	1 : 3260	1.4 : 1
COX-1 inhibition for a given IC _x COX-2::		
% Inhibition of COX-1 at IC ₅₀ COX-2	95.7 %	2.5 %
% Inhibition of COX-1 at IC ₈₀ COX-2	98.2 %	5.6 %
% Inhibition of COX-1 at IC ₉₅ COX-2	99.3 %	12.9 %
% Inhibition of COX-1 at IC ₉₉ COX-2	99.7 %	28.2 %

846 The data were obtained by the naïve pooled approach are reported